Engineering Electronic Lifetimes in Artificial Atomic Structures

K.-F. Braun and K.-H. Rieder

Institut für Experimentalphysik, Freie Universität Berlin, Arnimallee 14, D-14195 Berlin, Germany

(Received 14 September 2001; published 11 February 2002)

By means of atomic manipulation, 51 Ag atoms have been precisely positioned to form a triangle with a base length of 245 Å on a Ag(111) substrate. The scattering of the surface electrons at these adatoms results in a complex interference pattern. Spectroscopic data and dI/dV maps taken inside the triangle have been quantitatively evaluated by multiple scattering calculations of the wave pattern. Adjustment of the scattering parameters to the data yields the properties of the scatterers and the electron lifetimes. The experimental results for the electron lifetimes deviate from a $(E - E_F)^{-2}$ dependence and reflect the electronic band structure at the surface as well as the local influence of the triangle.

DOI: 10.1103/PhysRevLett.88.096801 PACS numbers: 73.50.Gr, 72.10.Fk, 73.20.At, 82.37.Gk

The determination of the lifetime of the surface state on noble metal surfaces has been the subject of experimental and theoretical work for a long time [1]. The lifetime of an electron is directly related to the phase-relaxation length L_ϕ, i.e., the distance an electron can travel without losing its phase information [2]. The lifetime, or equivalently the phase-relaxation length, plays a decisive role in the dynamics of surface chemistry [3] and quantum interference phenomena such as the Aharanov-Bohm effect or Friedel oscillations. The limiting processes for the lifetime of a surface electron are inelastic scattering with other electrons, inelastic scattering with phonons, as well as inelastic scattering and absorption at static structural defects such as step edges or adparticles.

On metal surfaces, electron lifetimes have been determined with different macroscopic techniques, in particular with high-resolution angule-resolved photoemission [1] and by femtosecond time-resolved two-photon photoemission experiments [4]. These techniques integrate over a macroscopic surface area with an unknown distribution of surface defects which are known to reduce lifetimes [5]. Scanning tunneling microscopy (STM), on the other hand, provides a means to probe the electronic properties of surfaces locally by scanning tunneling spectroscopy and dI/dV mapping. Applying these STM techniques to the Ag(111) surface, the lifetime of the surface state on a defect-free terrace has been determined at the dispersion minimum [6,7] by the evaluation of the linewidth of the surface state onset in tunneling spectra. In a different approach, the electron lifetimes have been measured with STM at energies above 1 eV [8]. To do so, the decay of quantum mechanical interference patterns from surface state electrons scattering off step edges has been investigated, which is influenced by the loss of coherence and hence by L_ϕ. Below this energy, the phase relaxation length becomes longer and longer and cannot be measured reliably from step edges anymore. But this limitation can be overcome by choosing a closed scattering geometry. Thereby each reflection contributes to a high total intensity which allows one to reliably resolve even small effects [9]. STM operated at a low temperature offers the possibility to manipulate single atoms and therefore to construct artificial structures several 10 nm in size. In the present work, the lifetime of the electrons inside such a quantum corral has been determined for the first time.

The experiments were performed with a homebuilt low-temperature UHV STM [10] at 6 K with a cut PtIr tip and the bias voltage V applied to the sample. As a first step the Ag(111) surface has been prepared by repeated sputter cycles at temperatures of 900 K. Preparing the sample at these high temperatures lowered the concentration of residual contaminants and adparticles by 1 order of magnitude down to 5×10^{-5} as compared to sputtering at room temperature. This low concentration is an indispensable condition for the kind of electron scattering experiments presented here, since a single scatterer on the surface can change the density of states even several hundreds of angstoms away and thus give undesirable contributions.

As a second step, Ag atoms were taken out of the surface by applying short voltage pulses to the tip [10]. By means of lateral manipulation, single Ag atoms were collected in a defect-free clean surface area and positioned precisely on the desired atomic positions. The atoms were moved in the pulling mode [10,11] using a sample voltage of +10 mV and a tunneling resistance of 50 kΩ. The Ag atoms were placed $5a_0 = 14.5$ Å apart along closed-packed row directions to form a triangle with a base length of 240 Å as is shown in Figs. 1(a) to 1(d).

The electrons of the surface state are scattered by the positioned Ag atoms, resulting in a standing wave pattern as can be seen in Fig. 1. Energy resolved data ranging from −55 to +796 meV with respect to the Fermi level were taken in the spectroscopic mode with the lock-in technique. For the lifetime determination, dI/dV maps were recorded in the constant-height mode, e.g., with a open feedback loop, since only then the dI/dV signal is in good approximation proportional to the local density of states (LDOS) of the surface. Above +262 meV the STM was operated with a closed feedback loop, because the topographic modulation becomes small at these energies and introduces only a negligible modulation through the height dependency of the transmission factor [12]. The measurements

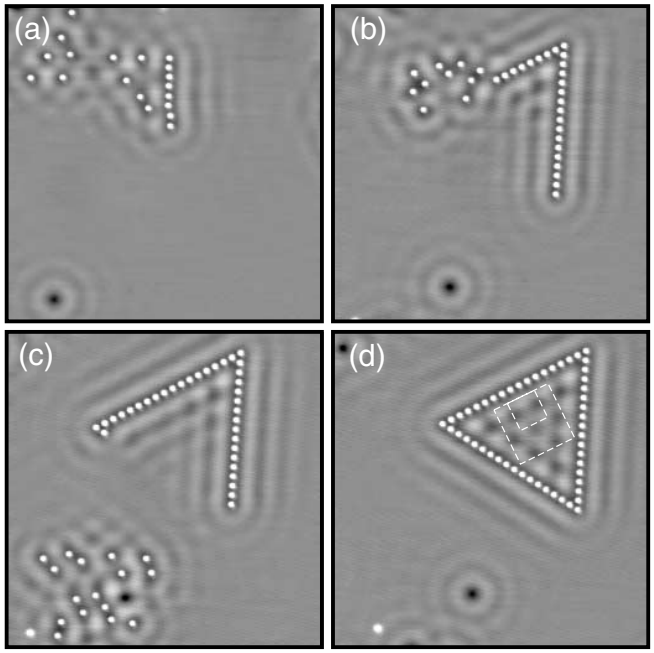

FIG. 1. Series of images showing the construction of the triangle consisting of 51 Ag atoms on a Ag(111) surface (49.3 nm × 49.3 nm, $U = +39$ mV, $I = 1.1$ nA).

were taken only inside the triangle (i) to avoid contact between the tip and the adatoms in the constant height mode, (ii) since the applied scattering theory does not describe the vicinity of the adatoms [13], and (iii) since the constructed rows of adatoms effectively screen the inside of the triangle against perturbations from its surroundings. For energies up to +262 meV the bigger and for higher energies the smaller rectangular area was chosen as shown in Fig. 1(d).

For the evaluation of the data, calculations of the wave pattern have been performed and the scattering parameters varied until coincidence with the measurements was achieved. The calculations are based on a multiple scattering approach [13] and include a model with only three physical parameters. The tip acts as a point source and emits a circular wave which is just a Hankel function, its value at the position of the adatom is $a_T(kr_i) = H_1^{(0)}(kr_i)$, where k denotes the wave vector, and r_i is the distance between the tip and adatom i. The scattering process at the point scatterers changes the phase of the incoming electron wave by a phase shift δ_i, and the amplitude of the electron wave can be decreased by inelastic scattering at the Ag atoms, which is expressed by the absorption α_i. Both scattering parameters enter the T matrix:

$$t_i = \frac{(\alpha_i e^{2i\delta_i} - 1)}{2}. \tag{1}$$

An Ag atom then emits an s wave, its value at a distance r is

$$a_T(kr_i)a_i(kr) = a_T(kr_i)H_1^{(0)}(kr)t_i. \tag{2}$$

This wave can then travel either directly or via further scattering processes back to the tip where it interferes with the emitted wave and the resulting intensity is detected. Within this model, the Schrödinger equation needs to be solved, and the solution including multiple scattering processes to infinite order is given by [13,14]:

$$\mathrm{LDOS} \propto \mathrm{Re}[\vec{a}_T^{\top} \cdot (1 - \tilde{A})^{-1} \cdot \vec{a}]. \tag{3}$$

Here $\vec{a}_T$ and $\vec{a}$ are vectors of the dimension N, the number of Ag adatoms, with values $a_T(kr_i)$ and $a_i(kr_i)$, and $\tilde{A}$ is an $N \times N$ matrix with $a_{ij} = a_i(kr_{ij})$ off-diadonal elements and zero diagonal elements.

Inelastic scattering processes between the scatterers lead to an additional spatially dependent decay of the electron amplitude which can be expressed with the phase-relaxation length L_ϕ as in [8]:

$$e^{-r/L_\phi}. \tag{4}$$

Here r denotes the distance between the tip and the Ag atoms or the distance between the Ag atoms, respectively. The phase-relaxation length L_ϕ can be simply transformed into an electron lifetime τ via $\tau = v_g L_\phi$; here v_g denotes the group velocity [15]. By adding this damping term to the electron wave function a many body property, e.g., the lifetime is approximately included in a single particle wave function. Since the lifetime is a local property, a mean lifetime is used in this model, averaged over the image area. At this point it needs to be emphasized that the inelastic scattering at the adatoms is described in the absorption α and the inelastic scattering between the adatoms independently in the phase-relaxation length L_ϕ.

As physical fit parameters only the phase shift δ, the absorption α, and the phase-relaxation length L_ϕ enter the calculations. The positions of the Ag atoms are fixed and exactly known, and for the dispersion of the surface state the dispersion minimum $E_B = -65$ meV and the effective mass $m^* = 0.4$ has been used [8,15]. Furthermore, values for the piezoconstants, the image position, and a small tilt angle between the plane of the tip movement and the surface plane have been included. By minimization of $\chi^2 = \Sigma(\mathrm{LDOS}_{\mathrm{calc}} - \mathrm{LDOS}_{\mathrm{data}})^2$ optimal agreement with the data was achieved as exemplified in Figs. 2(a) and 2(b). The difference between the recorded and the calculated image is shown in Fig. 2(c). The deviations at the left brim are due to the hysteresis of the piezos and have been excluded. Furthermore, small systematic deviations are observable which we attribute to a finite energy resolution and a small modulation of the topography due to the closed feedback loop at this energy. The width of the value distribution of Fig. 2(c) is shown in Fig. 2(d) and has been used to obtain an estimate for the standard deviation of the measurement points. The scale refers to the normalized values in Fig. 2(a) from −1 to +1. By then evaluating the formal covariance matrix error estimates of the fit parameters were calculated which take account of

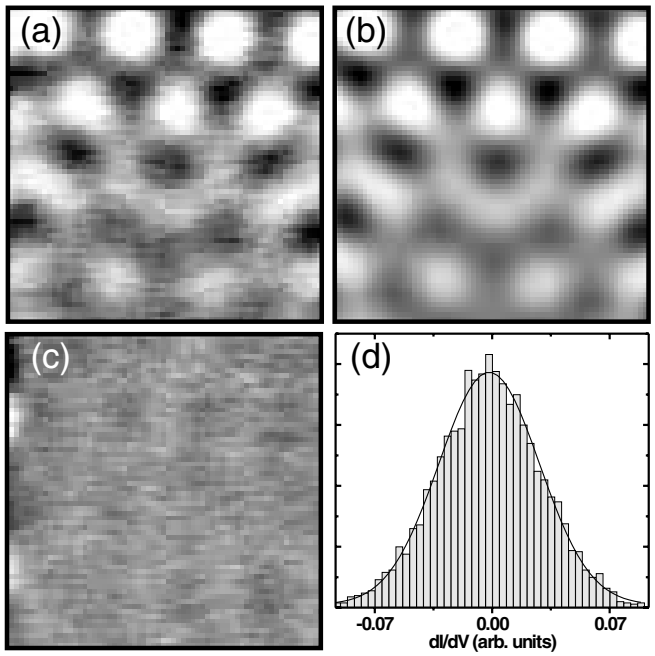

FIG. 2. (a) Data taken in the smaller rectangle of Fig. 1(d) at $U = +700$ mV. (b) This calculated image is the result after the adjustment of the model parameters to (a). (c) The difference image shows only minor deviations. (d) Value distribution of (c).

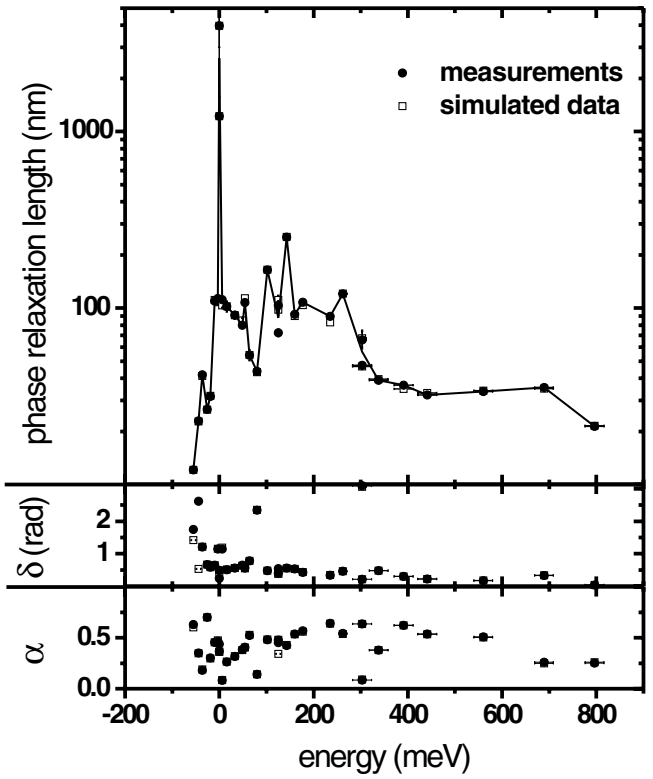

FIG. 3. The results of the adjustment of the calculations to the measured data are shown in this graph. The result for the simulated data proves the significance of the evaluation procedure.

statistical uncertainties of the data and cross dependencies between the fit parameter.

Figure 3 depicts the result of the calculations for the three physical parameters. To prove the significance of the evaluation procedure, repeated measurements would have to be performed which have been done for three energies. At these energies the results were reproduced within the error estimates. At the other energies, data with statistical noise was calculated and evaluated in the same manner. It can clearly be seen in Fig. 3 that over the whole range of energy the results are reproduced. This proves (i) the correctness of the error estimates and (ii) the negligible cross dependencies between the fit parameters.

The scattering parameters in Fig. 3 show only a weak energy dependence, and mean values of $\alpha = 0.43$ and $\delta = 0.24\pi$ have been derived. These values are close to $\alpha = 0.64$ and $\delta = 0.3\pi$ which were reported for Cu atoms on a Cu(111) surface [16]. There the authors have measured the pair distribution of the adatoms which interact through the surface state. Adjusting a simple model to their data yielded the above values. For the system Fe on a Cu(111) surface $\alpha = 0.0$ and $\delta = \pi$ have been reported [13].

For a discussion of the results the values of the phase relaxation length have been converted into lifetimes as shown in Fig. 4. The solid line denotes an extrapolation of the measurements in [8] taken above 1 eV, assuming a $\tau \propto E^{-2}$ law as predicted by Fermi liquid theory for a 2DEG [18]: Electrons injected at an energy E scatter inelastically with other electrons into unoccupied states with an energy smaller than E. The singularity at the Fermi energy is caused by the reduction of the number of available states to scatter into. The measurements clearly show a sharp maximum at this energy in accordance with theory. Furthermore, two pronounced edgelike features show up in the data at $+65$ and $+300$ meV as indicated in Fig. 4. Lifetime calculations as a function of energy for surface electrons have been carried out recently by Echenique *et al.* [17] for a Cu(111) surface. They showed that the intraband scattering within the surface state contributes to the electron lifetime at energies below the transition of the surface state into a surface resonance and even dominates at the dispersion minimum; this intraband contribution results in a reduced lifetime as compared to the $\tau \propto E^{-2}$ law valid at higher energies. The deviation sets in at about 15% below the transition of the surface state into the projected bulk states. For the Ag(111) surface, the lifetime has been calculated for the dispersion minimum only [7,17]. Thereby the calculated interband contribution describes also the lifetime at higher energies in agreement with experimental values [8]. The band structure of the Ag(111) surface [17] is depicted in the inset of Fig. 4. Assuming the onset of the intraband contribution to be 15% below the transition point results in the dashed curve in Fig. 4. From this argument we can clearly attribute the

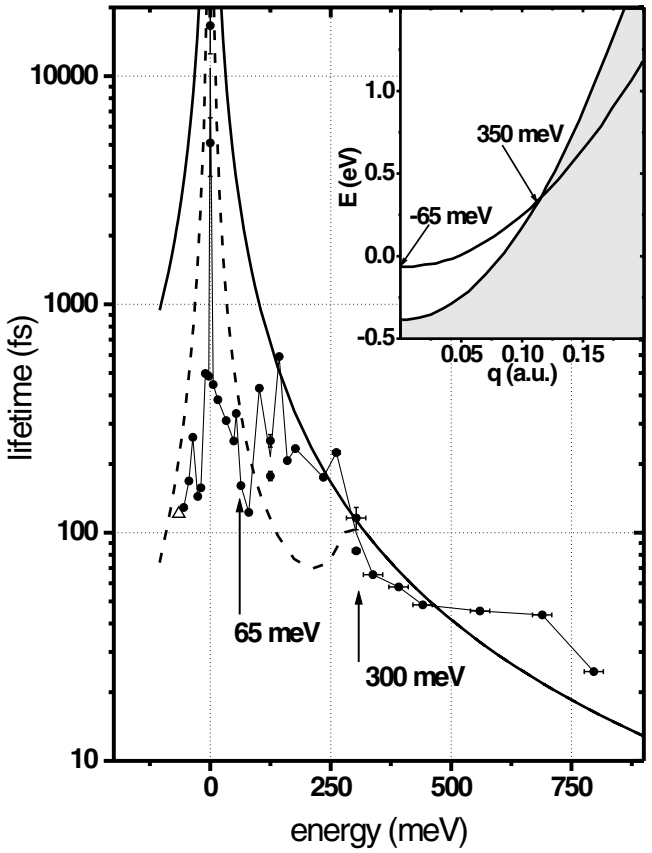

FIG. 4. The full circles connected by straight lines denote the measured lifetimes. The open triangle is a measured value on the defect-free terrace [6,7] and the solid line represents an extrapolation of the measurements in [8] taken above 1 eV. The dashed line is an adaptation to the theoretical calculation for Cu(111). The inset shows the dispersion of the surface state together with the projected bulk states [17].

pronounced edge at 300 meV to the transition of the surface state into the projected bulk states and thereby changing into a surface resonance. Another pronounced edge can be seen at +65 meV: Inelastic scattering of electrons injected at an energy E involves the excitation of electrons from occupied states at $-E$ (and up to the Fermi energy). Electrons excited from states below the dispersion minimum of −65 meV are bulk electrons and give only a small contribution to the lifetime [17]. Crossing +65 meV results in an enhanced scattering which gives rise to the observed edgelike feature. This is essentially the same situation as at +300 meV where the enhanced scattering is responsible for the observed edgelike profile. Finally, a fine structure can be observed which we have to attribute to the influence of the triangle. Clearly, this fine structure requires detailed theoretical investigations. Electron-phonon interaction gives a constant contribution independent of the energy except close the Fermi level where it becomes singular [19]. Furthermore, it is not sensitive to the dimensionality [7] and can therefore not explain the observed features.

In conclusion, the lifetime of the surface electrons in an artificial atomic structure has been measured for the first time. Future experiments should be performed on different substrates and a variety of species. The controlled atomic manipulation allows the design of arbitrary scattering geometries and, on the basis of a deeper understanding of the electron lifetimes, it should become possible to even engineer these lifetimes, which will become important in future nanoscale quantum devices.

The authors would like to thank R. Schrader and F. von Oppen for many helpful discussions.

Note added.—Upon acceptance of this manuscript, we became aware of similar work by Kliewer, Berndt, and Crampin [20].

[1] R. Matzdorf, Surf. Sci. Rep. **30**, 153 (1998), references therein.
[2] S. Datta, *Electronic Transport in Mesoscopic Systems* (Cambridge University Press, Cambridge, England, 1995).
[3] J. W. Gadzuk, Phys. Rev. Lett. **76**, 4234 (1996).
[4] M. Aeschlimann, M. Bauer, and S. Pawlik, Chem. Phys. **205**, 127 (1996).
[5] M. Weinelt, C. Reuß, M. Kutschera, U. Thomann, I. Shumay, T. Fauster, U. Höfer, F. Theilmann, and A. Goldmann, Appl. Phys. **68**, 377 (1999).
[6] J. Li, W.-D. Schneider, R. Berndt, O. R. Bryant, and S. Crampin, Phys. Rev. Lett. **81**, 4464 (1998).
[7] J. Kliewer, R. Berndt, E. V. Chulkov, V. M. Silkin, P. M. Echenique, and S. Crampin, Science **288**, 1399 (2000).
[8] L. Bürgi, O. Jeandupeux, H. Brune, and K. Kern, Phys. Rev. Lett. **82**, 4516 (1999).
[9] Although the falloff from a point scatterer is faster than from a step edge, the high number of scatterers in this experiment outweighs this opposed behavior.
[10] K.-F. Braun. Ph.D. thesis, Freie Universität Berlin, 2001.
[11] G. Meyer, L. Bartels, and K.-H. Rieder, Superlattices Microstruct. **25**, 463 (1999).
[12] J. Li, W.-D. Schneider, and R. Berndt, Phys. Rev. B **56**, 7656 (1997).
[13] E. J. Heller, M. F. Crommie, C. Lutz, and D. M. Eigler, Nature (London) **369**, 464 (1994).
[14] Y. Chan, Ph.D. thesis, Harvard University, 1997.
[15] Within experimental accuracy, no deviation from the unperturbed surface state dispersion has been found.
[16] J. Repp, F. Moresco, G. Meyer, K.-H. Rieder, P. Hyldgaard, and M. Persson, Phys. Rev. Lett. **85**, 2981 (2000).
[17] P. Echenique, J. Osma, M. Machado, V. Silkin, E. Chulkov, and J. Pitarke, Prog. Surf. Sci. **67**, 271 (2001).
[18] D. Pines and P. Nozieres, *The Theory of Quantum Liquids* (Benjamin, New York, 1966).
[19] L. Bürgi, H. Brune, O. Jeandupeux, and K. Kern, J. Electron Spectrosc. Relat. Phenom. **109**, 33 (2000).
[20] J. Kliewer, R. Berndt, and S. Crampin, New J. Phys. **3**, 22.1 (2001).